The Origin and Growth of K-Feldspar Megacrysts in Granodiorite, Tuolumne Intrusive Suite, California

Justine G. Grabiec and Allen F. Glazner, Department of Geological Sciences, University of North Carolina at Chapel Hill, CB# 3315, Mitchell Hall, Chapel Hill, NC 27599-3315; jgrabiec@live.unc.edu

Introduction

Importance: K-feldspsar megacrysts are common in granitic rocks and provide detailed physiochemical information about pluton crystallization, allowing us to understand how our continents are formed[1,2].

Problem: Two opposing hypotheses describe K-feldspar nucleation and result in different interpretations of igneous textures.

Hypothesis 1

- Based on large, euhedral crystal size and habit[3], crystals are interpreted to have nucleated in a hot, melt-rich, crystal-poor plutonic system[4,5,6].
- Successive melt replenishments from incremental pluton assembly homogenize melt. Crystals are lofted and churned, then settles[5,7] (Fig. 1).
- Low crystal numbers are due to nucleation difficulties[8].

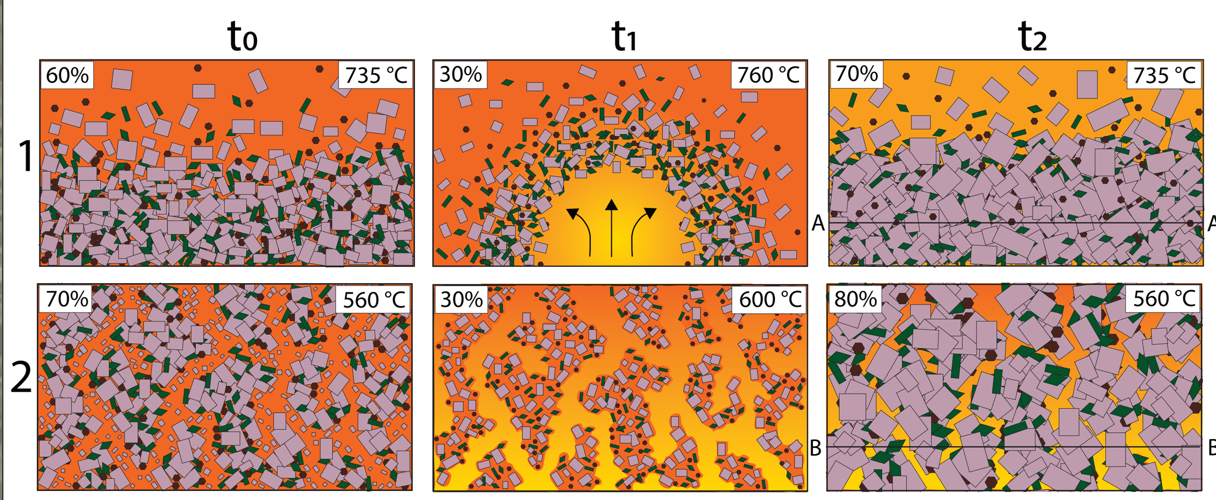

Figure 1. Schematic showing the magma chamber during both hypotheses. Percentages indicate crystallinity; temperatures indicate that of the system. t_0) Hypothesis 1: Cumulate formation via crystal settling[17]; Hypothesis 2: Static crystal matrix with channelized magma flow[16]. t_1) A new melt injection increases the temperature. In Hypothesis 1, the crystals are lofted and partially dissolved. The chamber churns and mixes, creating a new chemically homogeneous melt. In Hypothesis 2, a fresh melt injection flows through the channels while increasing matrix porosity by melting mineral rims. t_2) The system cools, awaiting another melt replenishment. In Hypothesis 1, the crystals settle to form another cumulate and have formed a rim of similar geochemistry. In Hypothesis 2, the crystals coarsen and maintain the static crystal matrix, an each crystal gains a new, geochemically unique, asymmetric rim. Transects (left) indicate the pattern we expect to see in a glacially eroded horizontal section of rock consistent with either hypothesis. Temperatures for Hypothesis 1 from [7] and Hypothesis 2 at t_0 and t_2 from [12] and at t_1 from [18,19,20].

Figure 2. Top: Megacryst mosaic in Tuolumne Intrusive Suite, Yosemite National Park. Bottom: Megacryst sample LP-4 cut parallel to c axis, revealing internal zoning.

Hypothesis 2

- Based on phase equilibria indicating K-feldspar nucleation at 50% crystallinity[7,9,10,11] in a relatively cool melt[12] and coarsening via dissolution-reprecipitation[13,14] as melt replenishments induce temperature oscillations[15].
- Mesostructures form as a static crystal matrix permits channelized magma flow[16] (Fig. 1).

Field Site

- Glacially eroded slabs in the Tuolumne Intrusive Suite (TIS; Fig. 3) reveal megacrystic mesostructures (Fig. 2).
- Biotite rinds surrounding megacrysts allow them to easily weather out of granodiorite.
- Two groups of Cathedral Peak Granodiorite megacrysts (Fig. 2) and one group of Half Dome Granodiorite phenocrysts (Table 1) were collected and analyzed.

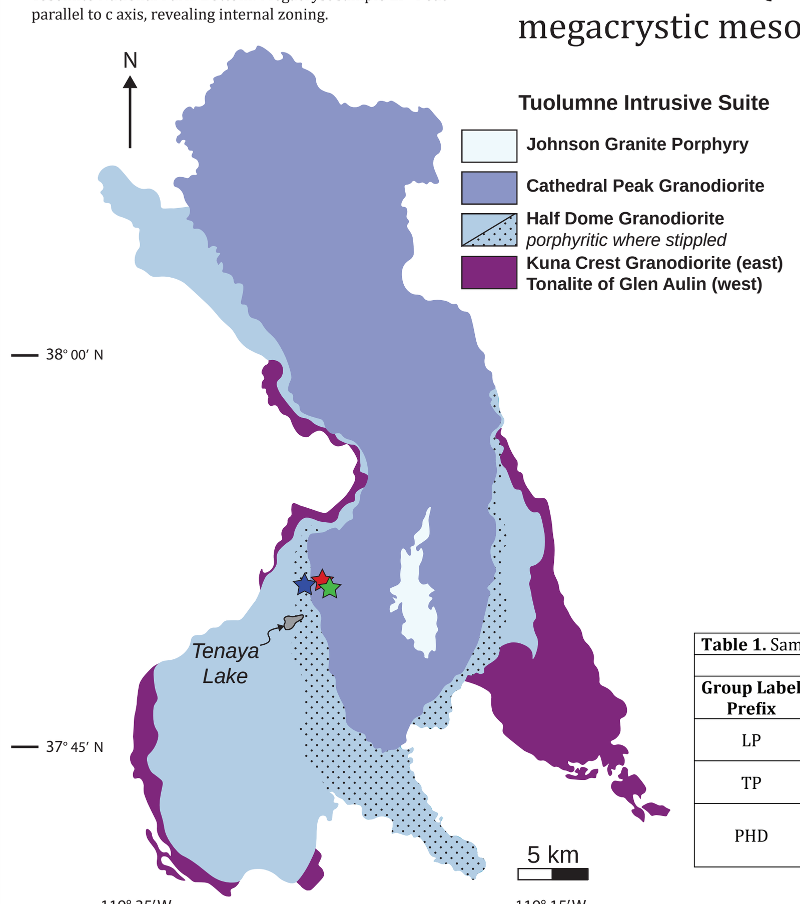

Table 1. Sample groups from TIS.

Group Label Prefix	TIS Geological Unit	Number of Samples	Sample Size Range (Length, mm)
LP	Cathedral Peak Granodiorite	10	51-79
TP	Cathedral Peak Granodiorite	6	40-56
PHD	Porphyritic Half Dome Granodiorite	6	30-34

Figure 3. Map of TIS after [15] and [21]. Red, green, and blue stars indicate sample locations for sample groups LP, TP, and PHD, respectively.

Methods

- Micro X-ray computed tomography scanning (Micro CT) can distinguish materials with different densities and can create three-dimensional models of megacrysts[22].
- Each scan is a collection of ~2,000 individual slices, which can be reconstructed for analysis of internal anatomy of each megacryst.
- Micro CT can resolve density differences between mineral inclusions as well as K-feldspar (2.56 g/cm³) and celsian ($BaAl_2Si_2O_8$; 3.32 g/cm³), making grayscale value a reliable proxy for Ba content of K-feldspar in high-resolution reconstructions.
- Ba zones in reconstructions were mapped by distinguishing between density differences (i.e., grayscale differences; Figs. 4, 5) in the K-feldspar.
- Two methods were used to analyze the maps: transect correlations and skeleton plots[23].

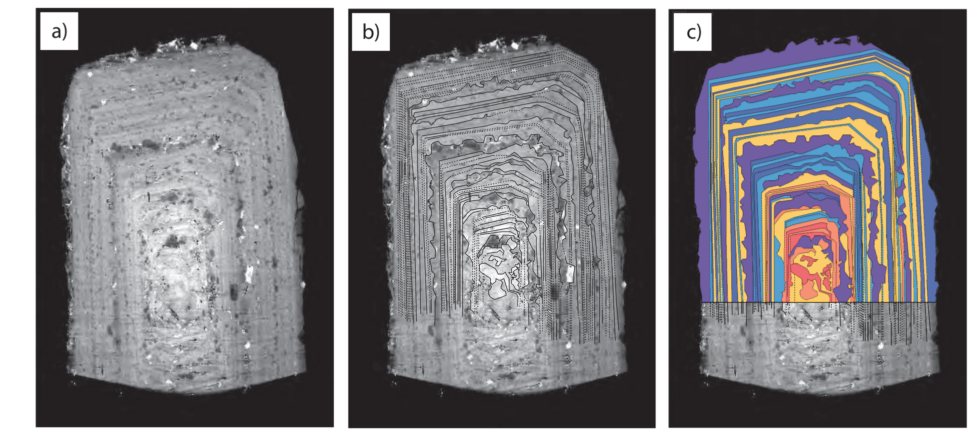

Figure 4. a) Reconstruction of LP-4, parallel to c axis. b) Outlined zones; solid lines indicate visible zone boundaries and dashed lines indicate inferred boundaries. c) Internally referenced map of zones based on Ba content (i.e., grayscale value). Red indicates highest relative Ba content (brightest gray) and purple indicates lowest relative Ba content (darkest gray).

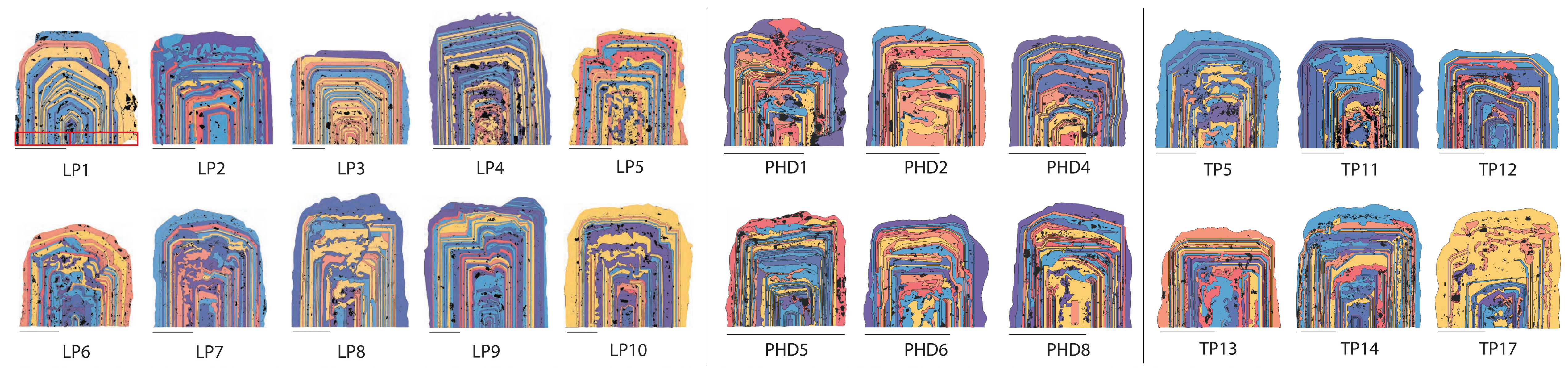

Figure 5. Internally referenced color maps of all three sample groups. Coloring is the same as that in Figure 4. Black spots indicate mineral inclusions. Black lines in lower left represent 1 cm scale. Red box on LP1 indicates location of mirroring transects selected in the same location for each megacryst.

Transect Correlations

- Transects (Fig. 5) were length-normalized and divided into 100 equidistant points.
- We recorded and translated the color of each point into a numerical dataset where purple equals 0 and red equals 5.
- The R^2 values of the datasets as compared to one another were calculated, including opposite transects from the same megacryst (Table 2).

Table 2. Sample groups and three highest R^2 values between randomly paired transects (including pairs from the same sample).

Sample Group	Highest R^2 Values
LP	0.34, 0.29, 0.24
TP	0.27, 0.18, 0.12
PHD	0.47, 0.32, 0.26

Skeleton Plots

- For each transect, the thickness and color (i.e., density and Ba content) of each zone were measured and plotted as a bar plot, which could be compared to one another to identify similar zone patterns in the same megacryst.
- Zones were kept in order but shifted to match similar portions of the transects from the same megacryst.

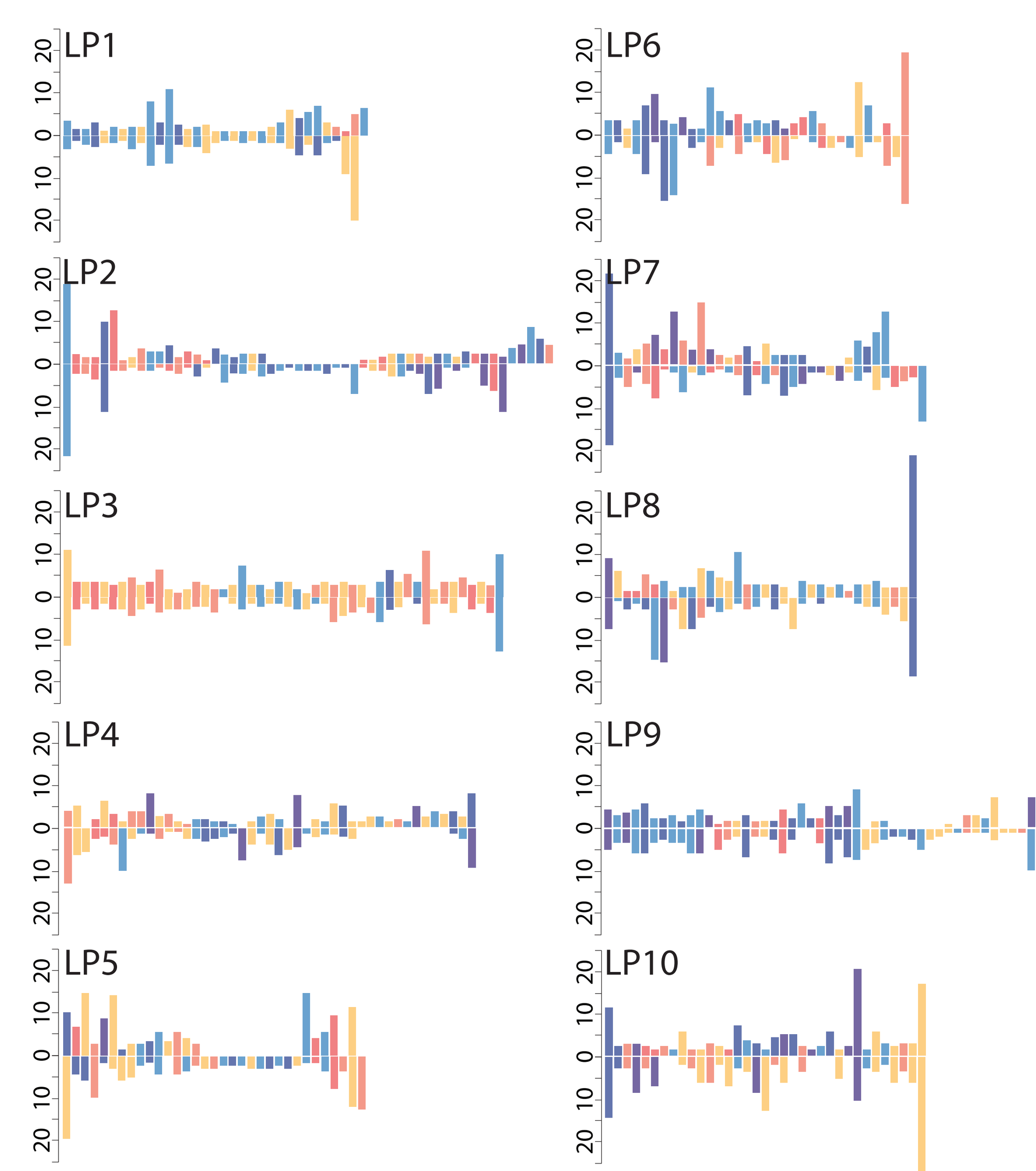

Figure 6. Altered skeleton plot pairs of transects from the same megacryst from sample group LP. The origin represents the core; the y axis represents the thickness of the zone in mm; each color corresponds to the color assigned to each zone in the color maps (Fig. 5).

Assumption 1: There are periods of dissolution or no crystallization.
Assumption 2: There are periods of time during which melts on either side of a crystallizing megacryst communicate and times during which they are separated.

- The mismatched skeleton plots from opposite transects from the same megacryst indicate that:
  1) Megacrysts crystallized in individual melt pockets in a static crystal matrix and formed subpockets as the melt crystallized, each with locally unique geochemistry.
  2) Pauses in growth indicate that dissolution-reprecipiation (Fig. 7) coarsened the megacrysts.
  3) For most transects there is an identifiable core where zones match, indicating nucleation of K-feldspar megacrysts in an igneous environment.
  4) A divergence from similar to different zone patterns indicates a transition from crystallization in a melt to coarsening via dissolution-reprecipitation.
- Mismatched zone patterns are also directly observable in the reconstructions (Fig. 8).

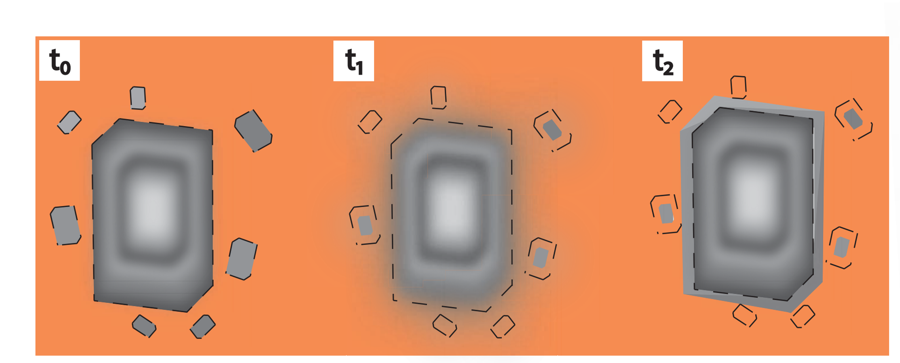

Figure 7. Dissolution-reprecipitation schematic during one temperature oscillation. Dashed lines represent original rims of crystals at t_0. t_0) A zoned K-feldspar megacryst surrounded by smaller crystals of variable Ba content. t_1) A temperature increase due to a melt replenishment dissolves the rims of the megacryst and larger surrounding crystals and entirely dissolves the smallest crystals. t_2) Dissolved chemical constituents recrystallize around the megacryst, decreasing the overall crystal number and size of the smaller crystals while coarsening the megacryst. Because the surrounding crystals vary in Ba content and because the freshly dissolved chemical constituents likely recrystallize on the nearest face of the megacrysts, interfingering zone patterns are produced.

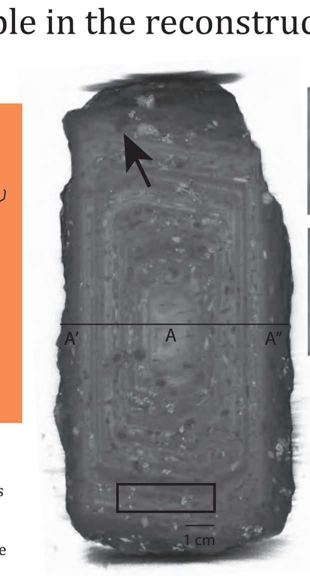

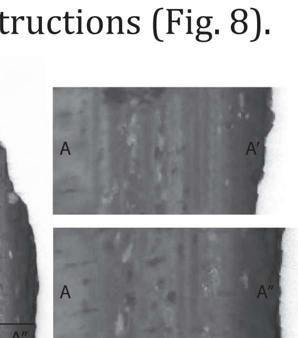

Figure 8. Transects from reconstruction of sample PHD4 showing similar but asymmetric zone patterns mirrored about the core. Arrow indicates an area of dissolution and the box indicates an area of interfingered zones.

Microstructures

- A variety of microstructures are evident in the megacryst reconstructions (Fig. 9).
- Dissolution features and interfingering of variable Ba concentrations (Figs. 9,10) in the same zone at a proportional distance from the core indicate that smaller crystals partly or wholly dissolved and contributed chemical constituents to the nearest large megacryst.

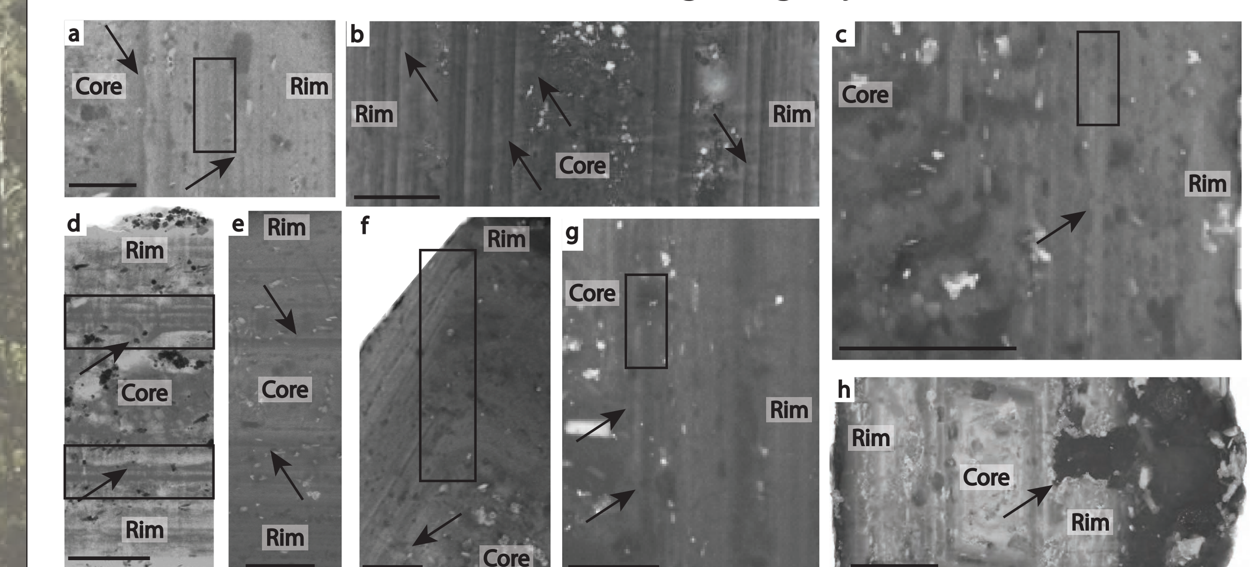

Figure 9 (Above). Microstructures observed in megacryst reconstructions. a) Sample LP9 with dissolution features (arrows) and oscillatory zoning (box). b) Sample TP14 with dissolution features (arrows) and sawtooth zoning. c) Sample LP6 with dissolution features (arrow) and interfingering zones (box). d) Sample TP13 with dissolution features (arrows) and oscillatory zoning (boxes). e) Sample LP7 with sawtooth zoning (arrows). f) Sample LP8 with dissolution features (arrow) and interfingering zones (box). g) Sample LP10 with dissolution features (arrows) and interfingering zones (box). h) Sample PHD1 with dissolution feature (arrow). Black line in lower left represents 5 mm.

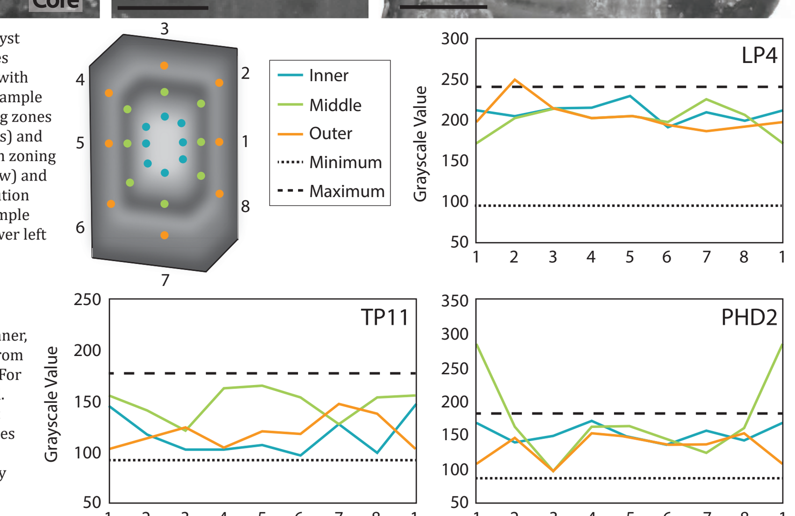

Figure 10 (Right). Internally referenced grayscale variations at proportional distances from the core for inner, middle, and outer zones of representative megacrysts from each sample group. The x axis represents spot number. For each spot, four measurements were taken and averaged. The minimum and maximum values represent the most K-feldspar-rich and the most celsian-rich grayscale values for the feldspar groundmass, respectively. Deviations outside of this zone of groundmass grayscale values may be due to sampling of mineral inclusions of different density than K-feldspar and celsian.

Conclusions

1) Ba zones in K-feldspar megacrysts are resolvable down to ~20 μm in Micro CT scans.
2) Maps of internal zoning are unique to individual megacrysts and imply that they crystallized in individual melt pockets with limited melt communication in a static crystal matrix.
3) Significant differences between zones on opposite sides of the same megacrysts indicate that at some point the static crystal matrix created subpockets from which unique zoning patterns on opposite sides of the megacryst formed. Opposite transects from the same megacryst are not significantly correlated.
4) Skeleton plots reveal identifiable cores that nucleated and crystallized in an igneous environment, followed by a divergence in zone patterns that indicate dissolution of outer zones and a move toward growth via dissolution-reprecipitation in a partly or wholly crystalline system (i.e., the cores are igneous, and the rims are meta-igneous to metamorphic).

References

[1] Ginibre, C., Wörner, G., and Kronz, A., 2004, Structure and dynamics of the Laacher See magma chamber (Eifel, Germany) from major and trace element zoning in sanidine: a cathodoluminescence and electron microprobe study: Journal of Petrology, v. 45, no. 11, p. 2197-2223. [2] Müller, A., Breiter, K., Seltmann, R., and Pécskay, Z., 2005, Quartz and feldspar zoning in the eastern Erzgebirge volcano-plutonic complex (Germany, Czech Republic): evidence of multiple magma mixing: Lithos, v. 80, no. 1-4, p. 201-227. [3] Johnson, B. R., and Glazner, A. F., 2010, Formation of K-feldspar megacrysts in granodioritic plutons by thermal cycling and late-stage textural coarsening, v. 159, no. 5, p. 599-619. [4] Tuttle, O. F., and Bowen, N., 1958, Origin of granite in the light of experimental studies in the system $NaAlSiO_8$-$KALSi_3O_8$-SiO_2-H_2O, Geological Society of America. [5] Luth, W. C., Jahns, R. H., and Tuttle, O. F., 1964, The granite system at pressures of 4 to 10 kilobars: Journal of Geophysical Research (1896-1977), v. 69, no. 4, p. 759-773. [6] Piwinskii, 1973, Experimental studies of granitoids from the Central and Southern Coast Ranges, California: Tschermaks mineralogische und petrographische Mitteilungen, v. 20, no. 2, p. 107-130. [7] Moore, J. G., and Sisson, T. W., 2008, Igneous phenocrystic origin of K-feldspar megacrysts in granitic rocks from the Sierra Nevada batholith: Geosphere, v. 4, no. 2, p. 387-400. [8] Vernon, R. H., 1986, K-feldspar megacrysts in granites—phenocrysts, not porphyroblasts: Earth-Science Reviews, v. 23, no. 1, p. 1-63. [9] Piwinskii, A. J., 1968, Experimental Studies of Igneous Rock Series Central Sierra Nevada Batholith, California: The Journal of Geology, v. 76, no. 5, p. 548-570. [10] Piwinskii, A. J., and Wyllie, P. J., 1968, Experimental Studies of Igneous Rock Series: A Zoned Pluton in the Wallowa Batholith, Oregon: The Journal of Geology, v. 76, no. 2, p. 205-234. [11] Whitney, J. A., 1988, The origin of granite: The role and source of water in the evolution of granitic magmas: GSA Bulletin, v. 100, no. 12, p. 1886-1897. [12] Ackerson, M. R., Mysen, B. O., Tailby, N. D., and Watson, E. B., 2018, Low-temperature crystallization of granites and the implications for crustal magmatism: Nature, v. 559, no. 7712, p. 94-97. [13] Mills, R. D., Ratner, J. J., and Glazner, A. F., 2011, Experimental evidence for crystal coarsening and fabric development during temperature cycling: Geology, v. 39, no. 12, p. 1139-1142. [14] Mills, R. D., and Glazner, A. F., 2013, Experimental study on the effects of temperature cycling on coarsening of plagioclase and olivine in an alkali basalt: Contributions to Mineralogy and Petrology, v. 166, no. 1, p. 97-111. [15] Coleman, D. S., Gray, W., and Glazner, A. F., 2004, Rethinking the emplacement and evolution of zoned plutons: Geochronologic evidence for incremental assembly of the Tuolumne Intrusive Suite, California: Geology, v. 32, no. 5, p. 433-436. [16] Higgins, M. D., 1999, Origin of megacrysts in granitoids by textural coarsening: a crystal size distribution (CSD) study of microcline in the Cathedral Peak Granodiorite, Sierra Nevada, California: Geological Society, London, Special Publications, v. 168, no. 1, p. 207-219. [17] Paterson, S. R., Vernon, R., and Zak, J., 2005, Mechanical instabilities and physical accumulation of K-feldspar megacrysts in granitic magma, Tuolumne Batholith, California, USA: Journal of Virtual Explorer, v. 18, no. 1, p. 1-18. [18] Carmichael, I. S. E., Turner, F. J., and Verhoogen, J., 1974, Igneous Petrology, New York, McGraw-Hill, 739 p. [19] Ernst, W. G., 1976, Petrologic Phase Equilibria, San Francisco, W.H. Freeman. [20] Glazner, A. F., and Johnson, B. R., 2013, Late crystallization of K-feldspar and the paradox of megacrystic granites: Contributions to Mineralogy and Petrology, v. 166, no. 3, p. 777-799. [21] Bateman, P. C., 1992, Plutonism in the central part of the Sierra Nevada batholith, California, 2330-7102. [22] Ketcham, R. A., and Carlson, W. D., 2001, Acquisition, optimization and interpretation of X-ray computed tomographic imagery: applications to the geosciences: Computers & Geosciences, v. 27, no. 4, p. 381-400. [23] Phipps, R. L., 1985, Collecting, preparing, crossdating, and measuring tree increment cores, US Department of the Interior, Geological Survey.

Acknowledgments

This project was funded by the University of North Carolina at Chapel Hill Department of Geological Science's Martin Trust and Geological Society of America Grant 12049-18. This work was performed in part at the Duke University Shared Materials Instrumentation Facility (SMIF), a member of the North Carolina Research Triangle Nanotechnology Network (RTNN), which is supported by the National Science Foundation (Grant ECCS-1542015) as part of the National Nanotechnology Coordinated Infrastructure (NNCI). Special thanks to Justin Gladman at SMIF for his assistance during Micro CT data collection and reconstruction. Thank you to Bryan Law, Drew Coleman, and the 2018 72H first-year seminar students for field assistance during sample collection.